

**CHAPTER 2**  
**BACKGROUND**

[MCours.com](http://MCours.com)

## **2.1 Atmospheric Ice Accretion on Outdoor Equipment**

Atmospheric ice deposition on outdoor equipment can adversely affect their operation or even result in serious and costly damages [1,37]. An example is the mechanical failure of power transmission lines and towers due to the static load of accreted ice, or dynamic stresses of ice shedding or wind-induced galloping [2]. It can also lead to loss of insulation [6-10] and electric arcs or flashovers between power lines and metallic supports, the latter being at ground potential. Wind loads can deteriorate the situation by intensifying the stresses on the mechanical parts. Engineers need to design the above structures with considerable margins to ensure their ability to withstand icing and windy conditions [38]. All these considerations increase the weight and cost of the infrastructures. Icing problem can impact many other systems such as ships, aircraft, vehicles, etc. Our interest here lies in the icing process in order to develop a method to reduce its adhesion to surfaces and eliminate related harmful effects.

### **2.1.1 Supercooled Water Drops**

Water drops can be cooled down much below bulk water freezing point ( $0^{\circ}\text{C}$ ). Figure 2.1 illustrates Levine's results [39] showing that tiny water drops may remain in liquid state below  $0^{\circ}\text{C}$  and their freezing point is size-dependent. For a water drop below the freezing point, commonly referred to as supercooled droplet, the liquid state is thermodynamically unstable. The most stable state for such droplets is the solid state which means an arrangement of water molecules in a lattice. This requires the movement of some molecules

and the gain of a higher degree of order, which is not favourable, according to the second law of thermodynamics. The net result is the lower freezing temperatures, seen in figure 2.1.

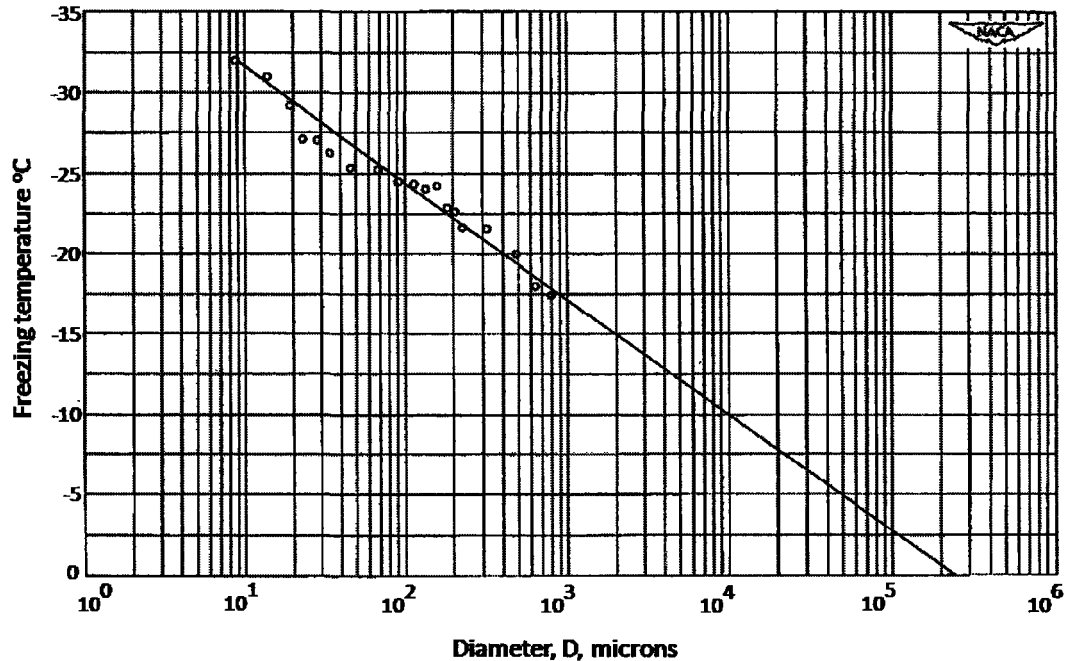


Figure 2.1: Freezing temperature of small water drops versus size [39].

The freezing process may be facilitated in presence of any substance acting as a freezing nucleus, which induces growth of an ice crystal about itself [40]. It is suggested that a material whose basal plane structure is similar to that of ice can be an effective nucleating agent [41]. Heterogeneous nucleation can take place by a variety of mechanisms. Theoretical studies and experimental measurements have shown that the ice nucleating ability of a particle is size-dependent and influenced by other physical and chemical factors [42]. This phenomenon could be seen in clouds or fogs above  $-30^{\circ}\text{C}$  where supercooled

droplets convert to ice particles through the presence of heterogeneous ice nuclei [43]. Levine in his studies also concluded that smaller droplets have less probability to contain nuclei, and therefore lower freezing temperature [39]. However, in clouds below  $-30^{\circ}\text{C}$  ice particles densities are more than ice nuclei densities [44] and it is believed that some supercooled water drops freeze homogeneously [45].

Both the heterogeneous and homogeneous nucleation phenomena inside the clouds are slow processes. For the objects in high altitudes, supercooled water droplets may impinge on exposed surfaces. An effective nucleus has a crystal structure similar to ice which allows water to crystallize by repeating its structure. Thus, the best nucleus for ice is a tiny piece of ice. That is why supercooled water droplets tend to rapidly join the ice layers covering the outdoor structures and objects.

### **2.1.2 Types of Atmospheric Icing**

Atmospheric icing appears when supercooled water drops approach the exposed surfaces of outdoor equipment. According to meteorological conditions, two types of ice formation could take place, namely in-cloud icing and precipitation icing. In-cloud icing occurs when the supercooled water droplets in a cloud come in contact with an exposed object. This kind of icing is relevant to the aircraft flying through clouds or the equipment installed high up in mountains.

Precipitation icing can happen in any place regardless of altitude during freezing rain. When a warm layer of air (above  $0^{\circ}\text{C}$ ) is trapped between two layers of cold air (below  $0^{\circ}\text{C}$ ), freezing rain may occur. Precipitation starts falling down as snow and reaching the

warm air, the snow particles melt to water. This water encounters the low-level cold air and becomes supercooled. Freezing drizzle has relatively smaller and lighter drops and originates from low level clouds whereas freezing rain is from higher clouds.

Atmospheric icing may arise as one of three types: glaze, hard rime and soft rime [46]. An alternative to them, wet snow, is of relatively less importance. Ice type is determined by supercooled droplet size, air temperature, wind speed, and properties of objects being hit by drops. The relationships of ice types with droplet size, air temperature, and wind speed are shown in figure 2.2, adopted from [47].

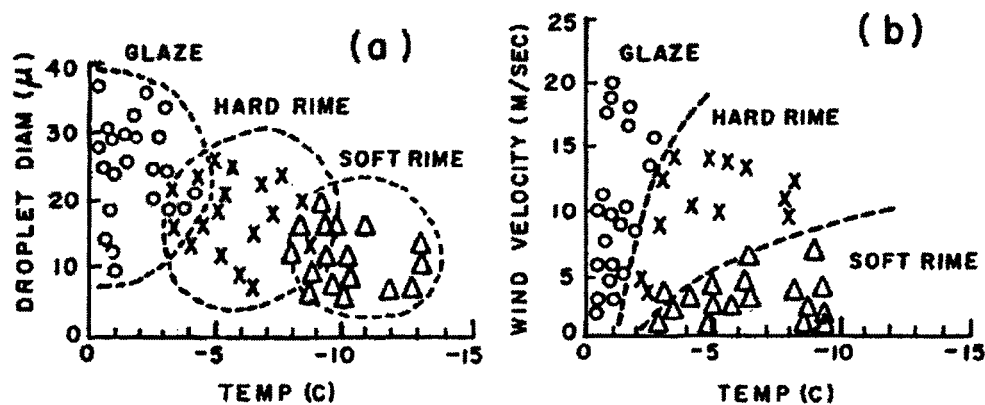


Figure 2.2: Atmospheric icing types as a function of (a) droplet diameter and air temperature, and (b) wind velocity and air temperature [47].

Glaze is a homogenous and transparent wet ice, depositing when relatively large supercooled droplets of freezing rain hit a subzero. Glaze accumulation happens at temperatures close to the melting point and under wet growth regime [48]. Lower temperatures create hard rime and soft rime. Rime ice accumulates when smaller supercooled droplets are in contact with dry objects below the freezing point [49]. This kind of ice mostly appears in mountains and at low wind speeds. Table 2.1 summarizes the

appearance, density, and formation conditions for each of the icing types. Among three types of atmospheric ice, glaze is denser and exerts larger static/dynamic forces to the equipment. Also it conducts electricity easier and is more dangerous for the performance of the components of electric networks.

**Table 2.1: Types and characteristics of atmospheric icing [50,51].**

Type of ice	Appearance	Density (g.cm-3)	Conditions of formation
Glaze	Hard, well-bonded, generally clear homogeneous ice	0.8-0.9	Supercooled water droplets at a temperature close to freezing (0 to -3° C) and wind speeds of 1-20 m/s
Hard rime	Hard, granular white or translucent ice growing along the direction of the wind	0.6-0.8	Supercooled water droplets at a temperature of -3 to -8° C, wind speeds generally 5-10 m/s
Soft rime	White, opaque, granular ice with delicate structure only loosely bonded, growing along the direction of the wind	< 0.6	Supercooled water droplets at a temperature of -5 to -25° C, and low wind speed (1-5 m/s)

### 2.1.3 Ice Adhesion

Ice forms strong bonds with the surface on which it freezes. The required stress to debond the ice from the surface is usually referred to as ice adhesion stress. Many parameters can influence the adhesion of ice to other materials. In addition to substrate properties, the conditions of ice formation can intensify the adhesion. Briefly, the adhesion is stronger when there is a lower freezing rate, more water on the material, higher droplet momentum, wider contact area, and lower air temperature down to a point.

The fundamental physics of ice adhesion is not well known yet. The bonds responsible for adhesion at the ice-solid interface are not unique. In [52] the authors divided the mechanisms of ice adhesion into the following categories:

- **Electrostatic:** There is evidence that some kinds of electron transfer [53] or proton ordering [54] happen at the interface of ice and solids, depending on the nature of material. These phenomena result in electrostatic attractions.
- **Diffusion and mechanical:** Penetration and diffusion of one material into the matrix of the other can help the materials adhere well. In presence of microscopic pores in a solid, a water drop can enter and freeze inside the pores. The expansion of water after freezing leads to a strong mechanical interlocking between the ice and substrate.
- **Chemical:** Materials adhere when chemical bonds are formed between them. Different types of bonding are likely to happen: hydrogen bonds, dipole-dipole bonds, dipole induced bonds, etc.

Chemical bonds are also of different types: electrical dipole-dipole interactions are intermolecular forces between polar molecules, such as water molecules. These forces are highly dependent on distance between the molecules and can be very strong when the molecules are close to each other. The attraction strength increases when polarity increases. Dipole- induced interactions (or Van der Waals forces) are mainly important for non-polar molecules and arise from temporary mismatch of electron clouds and nuclei. These weak forces act between all kinds of atoms or molecules. A hydrogen bond is an attraction interaction in which a hydrogen atom is attracted to two atoms (especially electronegative atoms) and acts like a bridge between them [55]. Usually, there is a considerable amount of oxides or adsorbed water molecules on the majority of practical solid surfaces, which can give rise to strong interaction with water molecules during freezing.

### 2.1.4 Ice Adhesion Measurement

Many investigators have studied the adhesion of artificial and atmospheric ice on various materials with a variety of surface properties [56,57]. Many methods have been used [58], for example, the techniques applying torsion shear, lap shear, cylinder torsion shear test, axial cylinder shear; methods such as cone test tensile, test, peel test or blister test [59], impact tests [21], laser technique [60], electromagnetic tensile tests [61], scratch tests [62] and so on. Each method was found to have its advantages and limitations.

The difficulty of reliable and meaningful ice adhesion measurements was reported long ago [63]. Some of the earliest studies on ice adhesion were carried out by Loughborough and Haas [64,65]. The shear strength of refrigerated ice was found to be about 1.72 MPa. Adhesion of artificial ice to metals was also measured to be from 0.85 MPa on copper to 1.52 MPa on aluminum. The authors noted a poor correlation between low ice adhesion and water repellency [64]. The adhesive strength of natural rime and glaze impact ice on aluminum power cables was studied by Phan et al. [66], Druetz et al. [67], and Laforte et al. [68], and the adhesive shear strength for hard rime was shown to vary 0.075 to 0.12 MPa. Both wind velocity and surface roughness appeared to increase the adhesive shear strength.

The first rotating centrifugal force method to measure adhesive strength of thin films of ice on metal was reported by Beams et al. [69]. Raraty and Tabor [70] also used the same technique to measure the adhesive shear strength of ice on polished-cleaned stainless steel. Stallabrass and Price [71] and Itagaki [72,73] used the rotating rod centrifugal method and found the adhesive shear strength of ice to be 0.03 to 0.07 MPa at  $-6^{\circ}\text{C}$ ; 0.03 to 0.16 MPa at  $-1$  to  $-15^{\circ}\text{C}$ . Kozitsokii [74] studied the effect of surface roughness on 304 SS plates. The



author considered three types of surfaces: a machined surface, a mat surface finish, and a mirror polish. Mean adhesive shear strengths were 0.6 MPa, 0.26 MPa, and 0.07 MPa respectively, for a snow-ice layer 0.1-0.2 cm thick. Thus surface roughness increased the shear strength by a factor of 10.

It is generally hard to compare the results of different ice adhesion values reported in the literature. Many parameters have to be considered when one tends to compare various investigations, for example ice formation conditions (e.g. airspeed, air temperature, droplet size, liquid water content, etc.), sample area and thickness, applied strain rate, and so on. Such substantial details are usually not mentioned clearly, or not reproducible. Strain rate has strong effect i.e. ice is ductile with viscoelastic behaviour at low strain rates, while brittle at high strain rates. The important issues in ice-adhesion measurement are reliability and reproducibility. An improved reproducibility of shear measurements requires uniformity in the force applied to the sample, enough ice-sample attachment area, and constant strain rate. One practical approach is to perform comparative or differential study; by applying ice both on known reference samples and on sample surfaces in completely similar way and then express the results in percent of change in shear strength.

### **2.1.5 Liquid-like Layer**

When the outermost layers of most solids approach the bulk melting temperatures, the molecular structure tends to a kind of disordered state with some attributes of both the solid

and liquid phases. It was found that on most of the ice interfaces a thin liquid or liquid-like layer (LLL) exists at temperature below the ice melting point [75,76].

One of earliest qualitative justifications of existence of such a layer and its extension to hundreds of molecular layers into the bulk was given by Weyl [77]. Following this report, various experimental methods were used to study the LLL, such as some dynamic measurements sensitive to the hydrodynamic properties of the layer (e.g., viscosity) [78], ellipsometry [79], photoelectron spectroscopy [80], nuclear magnetic resonance [81] and so on. Each of these experiments is based on a specific property of the LLL, so its thickness measurement can differ from the thickness measured by another approach. In addition to experimental investigations, many researchers tried to prove the existence of the LLL theoretically. For a brief list one can refer to [82].

A common observation in different experiments is temperature dependence of LLL. The thickness of the LLL increases rapidly as temperature rises. As shown in figure 2.3 having the temperature near bulk melting point, the thickness of the LLL increases rapidly up to micrometer scale. This is the temperature range in which glaze, the most bothering atmospheric ice, is most likely when precipitation drops are large and wind is strong. If one can find a surface coating capable of repelling water (and thus probably the LLL), such a coating is expected to effectively reduce ice adhesions and/or accumulation. Superhydrophobic materials show very low affinity to water, and are good ice-repellent candidates, as discussed in the following section.

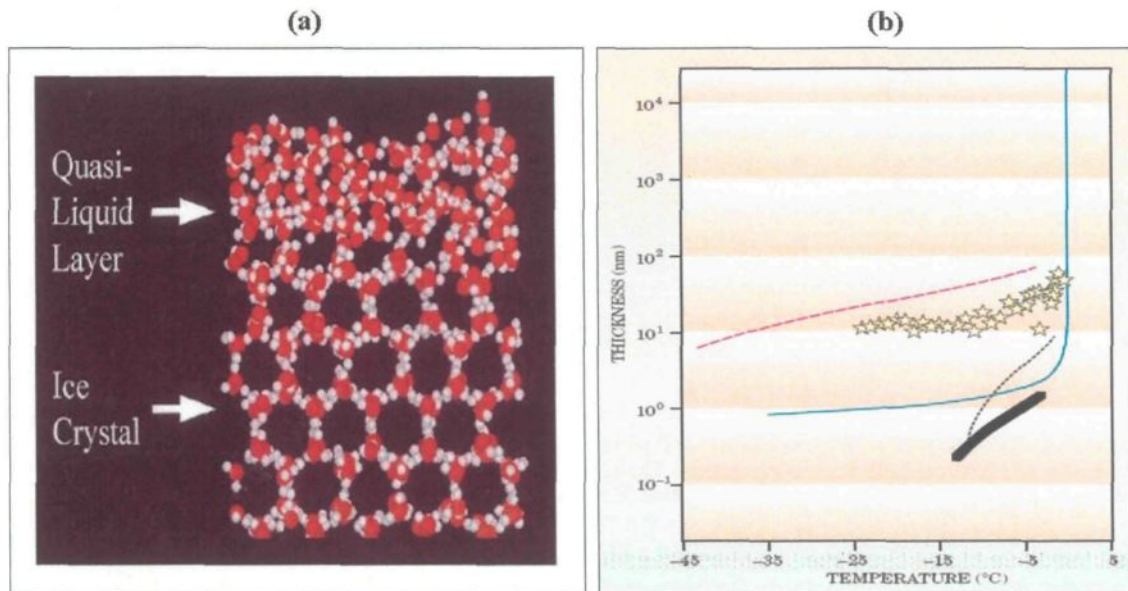


Figure 2.3: (a) Molecular dynamics simulation of the LLL structure at 265K, (b) the thicknesses of the LLL by proton backscattering (red dashed line) [83], x-ray scattering using a glass interface (black dashed line) and a silicon interface (black bold line) [84,85], AFM (stars) [86] and relegation (blue solid line) [87]

## 2.2 Wettability and Superhydrophobicity

### 2.2.1 Surface Energy and Surface Tension

Although plasma is the most abundant phase of matter in the world, in our daily life we face the other three familiar states; solid, liquid and vapour. Wetting phenomena happen in the points where all the three states are in contact. In other words, wetting includes the behaviour of intersection of three interfaces, solid-liquid, solid-vapour, and liquid-vapour.

An interface is the boundary between two phases, and when one side is a vapour or gas, the other is called a surface. The properties of surfaces are different compared to the

interior or bulk. One important aspect is the extra energy associated with the surfaces, also known as surface energy. When a solid material is cleaved to two pieces, the applied energy is used to break the chemical bonds between the atoms of the material and the conservation of energy results in the increment in energy of these atoms. The energetic atoms tend to reduce their energy, so they undergo relaxation (a slight rearrangement in surface layers) and reconstruction (displacements of the surface atoms) as well as adsorption and oxidation in presence of air. But the surface energy remains still high. For liquids, it is common to use the term of surface tension, a vector quantity, instead of surface energy, both having a dimension of force per unit length ( $\text{Nm}^{-1}$ ) or energy per unit area ( $\text{Jm}^{-2}$ ). In the case of liquids, the unfavourable surface energy is lowered by minimizing the amount of exposed area and also by surface relaxation [88]. The direction of surface tension is inward the liquid, determining the curvature of free surfaces of liquids, rising the liquids in tiny vertical pipes and wetting the solid surfaces. The measured surface tensions of some common liquids are listed in appendix A.

For crystalline materials, many of physical and chemical properties are directional and dependent on the microstructural attributes. Surface energy of metals has been subject of numerous theoretical [89,90] and experimental investigations [91]. Appendix B includes the values of surface tension for some common metals. For more complete list one can refer to [92].

### 2.2.2 Contact Angle as Wettability Indicator

Wetting occurs when a liquid drop contacts a solid surface. As a result, fractions of both the liquid surface and solid surface are reduced while a solid-liquid interface appears. For a given solid, a low-surface-tension liquid will spread easily while a high-surface-tension one tries to keep its drop shape. Similarly for a given liquid, a high-surface-energy solid tends to be covered (or wetted) in contrast to low-energy surface one which does not absorb the liquid. If the liquid does not spread to make a thin layer, it will sit as a spherical-cap-like droplet.

The most common quantitative indicator of wettability is contact angle. It is believed that contact angle measurement is a reliable method to study the surface energy. The contact angle value for ideal surfaces (smooth, planar, homogenous and rigid),  $\theta_0$ , is given by Young's equation [93]

$$\cos\theta_0 = \frac{\gamma_{SV} - \gamma_{SL}}{\gamma_{LV}} \quad (\text{Eq. 2.1})$$

where  $\gamma_{SV}$ ,  $\gamma_{SL}$  and  $\gamma_{LV}$  are surface tensions for the solid-vapour, solid-liquid and liquid-vapour interfaces, depicted in figure 2.4.

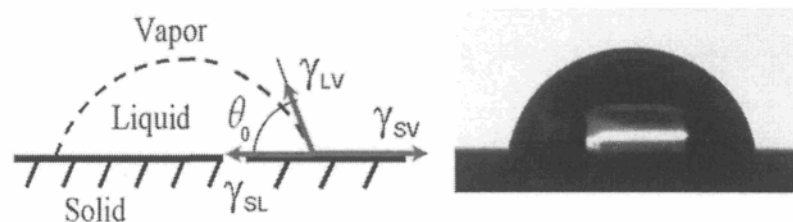


Figure 2.4: Interfacial tensions and contact angle.

Young equation gives the contact angle which corresponds to minimum energy of a drop on a smooth solid surface [94]. In this equation, the solid surface is considered as a hard homogenous material which doesn't reshape or dissolve and there is no liquid penetration.

When the selected liquid is water and  $\theta_0 < 90^\circ$ , the solid is named hydrophilic (having a substantial affinity for water) and for  $\theta_0 > 90^\circ$  the solid is hydrophobic (lacking affinity for water). Actually, hydrophobic materials attract water but the tendency between water and material molecules is weaker than between water molecules. In the extreme case of hydrophilicity,  $\theta_0 = 0^\circ$ , water wets the entire surface and spreads completely to form a thin layer. On the other hand, the surfaces with contact angles more than  $150^\circ$  are called superhydrophobic or ultrahydrophobic.

### 2.2.3 Contact Angle Measurement

The different methods applied to measure the contact angles can be categorized into two main groups based on the state of droplet during procedure:

- Static: the drop is placed on the surface before measurement and its volume is momentarily constant while the contact angle is measured.
- Dynamic: the contact angle is studied when the drop is being enlarged, reduced or moved. The boundary of liquid-solid interface is evolved during the measurement process.

Static methods can give the values of equilibrium contact angles. A liquid droplet of 3 to 8  $\mu\text{L}$  is placed on the surface and the needle is removed so that the drop can take its shape freely without any alteration due to presence of needle. The condition of constant volume of drop is required temporarily for measuring the contact angle and does not mean that the volume is kept constant continuously. Many events may alter the drop volume, such as liquid evaporation, dissolving the solid in to liquid or vice versa, chemical reaction between the solid and liquid and so on. Sometimes, the time-dependent evolution of droplet on the surface can provide useful information and usually there is a facility in measuring systems to record the variations of contact angle versus time.

Dynamic contact angles describe the evolution at the liquid-solid boundary during the wetting and de-wetting processes. The main purpose of dynamic method is to achieve the advancing and receding contact angles. During the process the needle remains in the drop throughout the whole measurement so the selection of proper size is important to have the results not affected by the presence of needle. When there is a relative displacement between solid surface and needle the velocity should be selected properly. A reliable and stable boundary is not formed instantaneously but needs some time before equilibrium is reached. The similar argument is correct when there is a liquid injection or suction to alter the drop size. The needle diameter, droplet size and injection rate should be selected precisely.

Another dynamic method for contact angle measurement is by tilting the solid surface. The solid surface is slowly tilted from horizontal state and the contact angles are constantly measured. The acceptable contact angle is the one just before the drop starts to roll. The

inclination angle of surface with horizontal plane is called sliding angle. It is worth mentioning that this procedure is highly dependant to the size of liquid droplet. Each method has it advantages and limitations and the proper method should be selected according to the actual experiment.

### 2.2.4 Contact Angle Hysteresis

Young's equation predicts a unique value for contact angle, but in reality a liquid drop on a solid does not show just a single contact angle. If a drop is placed on a static horizontal solid surface, the contact angle is named as sessile. When there is a relative movement between the droplet and the surface, for instance because of tilting, as in figure 2.5, there will be a change in the contact angles. Another example is when the volume of droplet increases or reduces because of injecting/sucking the liquid to/from droplet with a needle. The contact angles at the wetting and de-wetting edges of droplet are called as advancing and receding, respectively. Usually the sessile contact angle is greater then receding angle,  $\theta_R$ , and less than advancing angle,  $\theta_A$ .

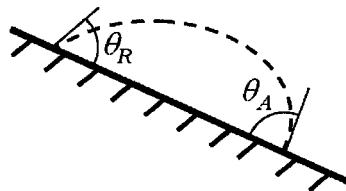


Figure 2.5: Advancing and receding contact angles of a liquid drop on a tilting solid surface.



Experiments have shown that the hysteresis is related to the chemical and structural heterogeneity of the surface [95-98]. However, there is almost no unique relation between the values of contact angle and contact angle hysteresis. In other words, it is normal to have surfaces with a similar contact angle value but with quite different hysteresis numbers. On the other hand, low hysteresis usually happens when the sessile contact angles are large, i.e. in superhydrophobic materials. Hysteresis is a very important property and should be considered precisely when the ease of liquid movement on the surface is concerned.

### **2.2.5 Passivation**

The surface energy of solids is a surface property, which means it is determined by few outermost atomic layers. Therefore, the energy of a particular surface can be increased or decreased by covering the surface with an appropriate thin film, usually as thin as a few layers of molecules. When the final energy is lower than original value, the process is called a passivation.

Some organic molecules have a polar group at one end (namely head) and a non-polar long saturated hydrocarbon chain on the other end (tail). Since the hydrocarbon chain has all its valence requirements satisfied by carbon-carbon or carbon-hydrogen bonds, it is fairly inert to the polar interactions with polar liquids like water. The polar head can be absorbed to other polar molecules or to high energy solid surfaces and make bonds. In ideal case, the entire solid surface can absorb enough number of these organic molecules and be covered perfectly with only one molecular layer. This ordered arrangement of molecules is called self-assembled monolayer, or SAM. Presence of such a molecular layer can result in

considerably lower surface energy. SAMs have been subject of intensive studies and many organic acids with saturated long chains or alkylsilanes are found to form SAMs [99-101] .

Fluorine, the first element of seventh group in periodic table, is known to be effective for lowering the surface energy. A variety of fluorinated materials have been prepared with excellent resistances against water, oil and organic solvents, for example polytetrafluoroethylene (PTFE) with more familiar name, Teflon. According to the functional groups, the surface energy reduces in this order:  $-\text{CH}_2 > -\text{CH}_3 > -\text{CF}_2 > -\text{CF}_2\text{H} > -\text{CF}_3$  [102]. The least surface energy relates to the hexagonal arrangements of closely packed  $-\text{CF}_3$  groups [103]. Some types of fluorocarbon SAMs showed promising to reduce ice adhesion compared to bare aluminum surfaces [104,105]. This is also compatible with theoretical predictions [28]

### 2.2.6 Effect of Roughness, Superhydrophobicity

The passivation is not the only parameter which can affect the wettability of materials, the surface morphology is equally important. Usually, passivated smooth solids show the maximum achievable contact angles  $\sim 120^\circ$ , quite far from the maximum value of  $180^\circ$  [106]. On the other hand, there are some plants in nature, such as *Nelumbo nucifera druce*, which exhibit very high water contact angles (CA) and very low contact angle hysteresis and this property is usually known as the Lotus Effect [29], as shown in figure 2.6a. This phenomenon is not restricted to plants. Similar properties are identified in some animals and insects. It is worth mentioning that lotus leaves are covered by a paraffinic wax containing predominantly  $-\text{CH}_2-$  groups [29]. In lotus leaf surfaces, lower energy of  $-\text{CH}_3$

groups or fluorocarbons are not present and the surface energy is not extremely low [107]. The key feature of these natural surfaces, which makes them so water-repellent, is the presence of a specific surface morphology. In figure 2.7 some scanning electron microscopy (SEM) images of these tissues are shown [108].

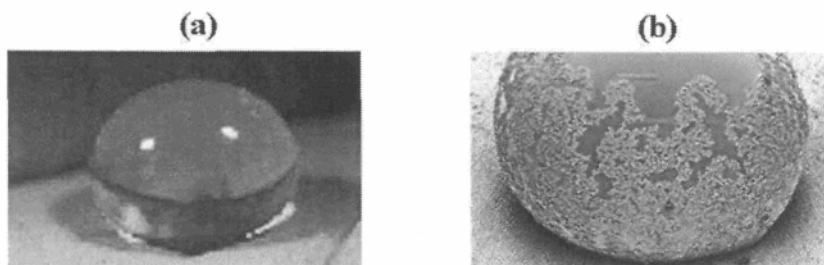


Figure 2.6: (a) water drop on lotus leaf with contact angle more than  $150^\circ$ , (b) self-cleaning property of lotus leaves

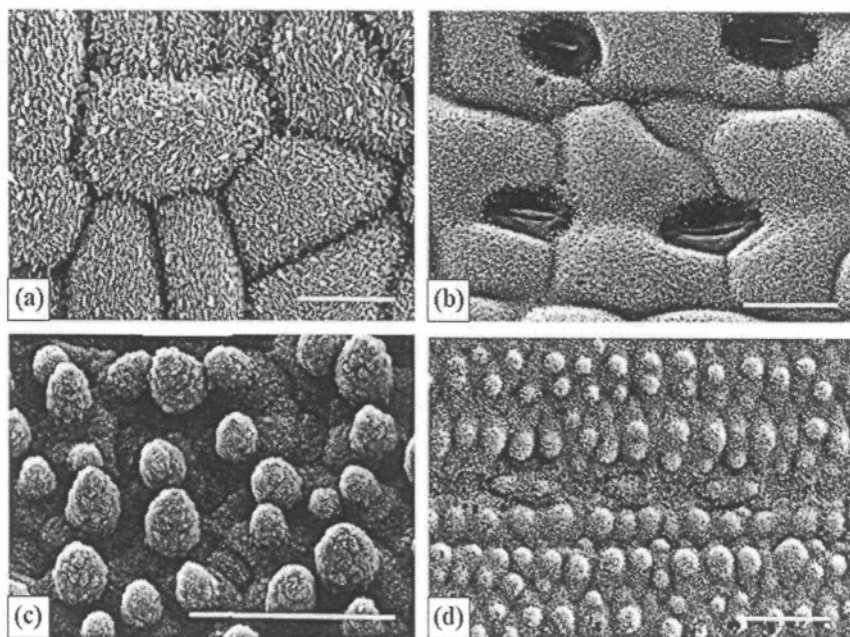
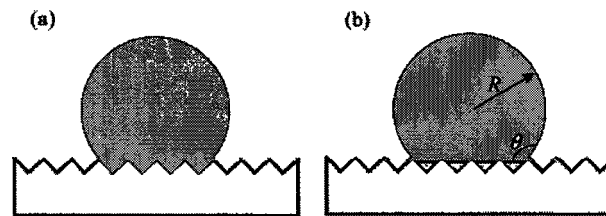


Figure 2.7: SEM images of superhydrophobic leaf surfaces. Water-repellent leaf surfaces of (a) *hypericum aegypticum*, scale bar= $20\mu\text{m}$ ; (b) *mMarsilea mutica*, bar= $20\mu\text{m}$  (c) *nelumbo nucifera*, bar= $50\mu\text{m}$ . (d) *sinarundinaria nitida*, bar= $20\mu\text{m}$ .

When the sessile contact angles are over  $150^\circ$ , the surface is usually termed as superhydrophobic [26]. Natural superhydrophobic materials usually have a very low hysteresis which appears in simplicity of rolling the water drops off the surface. The rolling droplets absorb the dust and debris and carry them out of the surface, as depicted in figure 2.6b. This is called self-cleaning.

On a rough solid surface, the predicted contact angle by Young's equation,  $\theta_0$ , may be not close to the measured contact angle. When the surface is rough, two distinct events may happen: liquid can completely fill up the grooves (figure 2.8a) or some air bubbles entrap underneath the liquid (figure 2.8b). The former situation is the "homogeneous wetting regime", while the latter is the "heterogeneous wetting regime" [109].



**Figure 2.8: Liquid drop on rough hydrophobic surface: (a) homogenous (Wenzel) and (b) heterogeneous (Cassie-Baxter) regimes**

Wenzel [110] introduced an equation defining a relation between the actual contact angle on rough surface in homogenous wetting regime and the Young's contact angle as follows:

$$\cos \theta^W = r \cos \theta_0 \quad (\text{Eq. 2.2})$$

where  $r$  is the roughness factor defined as the ratio of the actual area of a rough surface to the projected area. If  $\theta_0$  is less than  $90^\circ$ ,  $\theta^W$  is smaller than  $\theta_0$  and reduces as  $r$  increases.

On the other hand, when  $\theta_0$  is greater than  $90^\circ$ ,  $\theta^W$  is greater than  $\theta_0$  and increases by increment of  $r$ . Figure 2.9 shows the effect of roughness in Wenzel model for a range of  $r$  and  $\theta_0$ . Therefore, based on Wenzel model it is impossible to have the contact angles in the shaded areas in figure 2.9a. Another limitation of Wenzel model is no prediction for  $\theta^W$  in the cases of  $r \cos \theta_0 > 1$ .

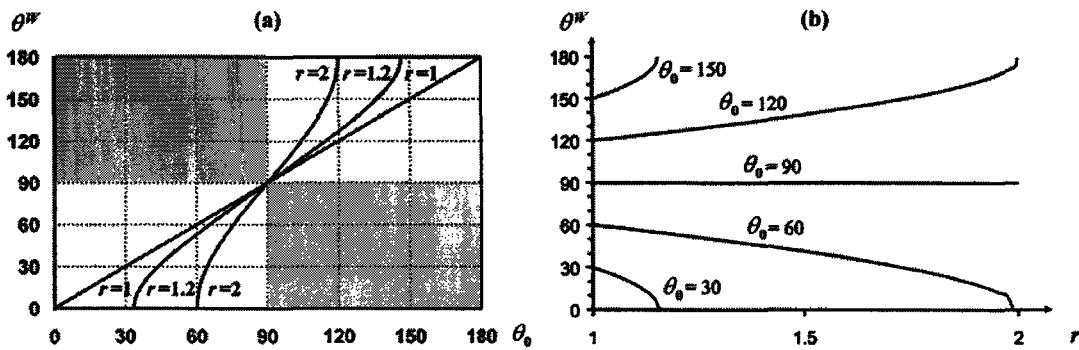


Figure 2.9: (a) Contact angles predicted by Wenzel's model for roughness factors of 1, 1.2, and 2 [98]; (b) contact angle for rough surface as a function of roughness factor in Wenzel's model [111]

All surfaces have some degree of chemical heterogeneity. A heterogeneous solid surface has domains with different surface free energies. Cassie and Baxter [112] developed another model by considering the interface composed of two types of domains: fraction  $f_1$  with contact angle of  $\theta_1$  and fraction  $f_2$  with contact angle of  $\theta_2$  where  $f_1 + f_2 = 1$ . The predicted contact angle,  $\theta^{CB}$ , can be calculated as:

$$\cos \theta^{CB} = f_1 \cos \theta_1 + f_2 \cos \theta_2 \quad (\text{Eq. 2.3})$$

It states that the cosine of the contact angle on a heterogeneous surface is the weighted average of the cosines of the contact angles on the various fractions. In the case of rough heterogeneous surfaces, it is possible to have some amount of air entrapped beneath the liquid drop. If fraction  $f_2$  represents the solid-air interface and considering that liquid drops in air have spherical shape, or equally  $\theta_2 = 180^\circ$ , we have:

$$\cos\theta^{CB} = f_1 \cos\theta_1 + f_2 \cos\theta_2 = f_1 \cos\theta_1 + (1 - f_1) \cos 180^\circ = f_1 \cos\theta_1 + f_1 - 1$$

where  $f_1$  is solid-liquid fraction. Replacing  $f_1$  with  $f$  and  $\theta_1$  with Young's contact angle  $\theta_0$  lead to:

$$\cos\theta^{CB} = f \cos\theta_0 + f - 1 = f(\cos\theta_0 + 1) - 1 \quad (\text{Eq. 2.4})$$

known as modified Cassie-Baxter model [113,114]. Having this model, it is possible to obtain  $\theta^{CB} > 90^\circ$  even if  $\theta_0 < 90^\circ$ , provided that  $f$  is very small. Figure 2.10 depicts the effect of roughness in modified Cassie-Baxter model for a range of  $\theta_0$  and some  $f$  values.

Another form of Cassie-Baxter model is also suggested as:

$$\cos\theta^{CB} = r_f f \cos\theta_0 + f - 1 \quad (\text{Eq. 2.5})$$

where  $r_f$  is roughness ratio of wet area of solid [109]. This equation gives more precise contact angle because of considering the effect of the curvatures in wet area. It is known that both the Wenzel and Cassie-Baxter models can be correct only if the drop size is sufficiently large compared with typical surface roughness [115,116].

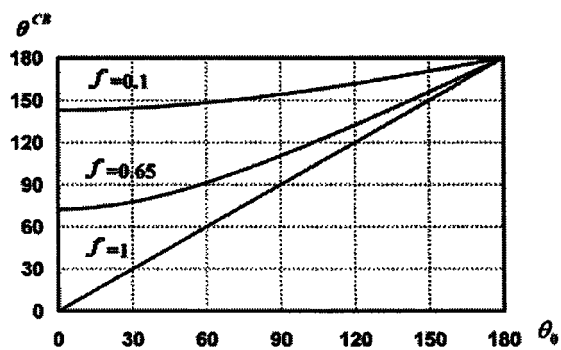


**Figure 2.10: Contact angles predicted by the modified Cassie-Baxter model for solid-liquid fractions of 0.1, 0.65, and 1 [98].**

Homogeneous and heterogeneous wetting regimes are commonly referred to as Wenzel and Cassie-Baxter wetting regimes. Many researchers tried to find out which of the wetting regimes is preferred for drops in equilibrium state on certain surfaces [117,118]. It is found that transitions are probable between wetting regimes in superhydrophobicity and there is a relationship between the solid surface topography and the transition between the homogeneous and heterogeneous wetting regimes [118].

### 2.2.7 Artificial Superhydrophobic Surfaces

In many areas of technology it is required to control the wettability of surfaces. Self-cleaning property is desirable for car windshields, aircraft, solar energy cells, etc. A general classification of methods to prepare superhydrophobic surfaces into two broad groups is given in [107]. The former group includes the ways of roughening the low-surface-energy materials and latter one has the two-step methods; making a rough surface and then passivating it. A brief of each category is as follows:

### **Roughening a low surface energy material:**

- **Fluorocarbons:** Fluorinated polymers have extremely low surface energies. Roughening these polymers can lead to superhydrophobicity. For example, one can name achievement of 165° water contact angle on PTFE by Zhang et al. [119], 161° on polymer-embedded PTFE by Menini et al [120], 159° on poly[bis(2,2,2-trifluoroethoxy)phosphazene] by Singh et al. [121], etc. **Silicones:** Polydimethylsiloxane (PDMS) is a well-known material with low surface energy that can readily be converted into superhydrophobic surfaces. Some works on PDMS are reported with water contact angles up to 175° by Khorasani et al. [122], 160° by Jin et al. [123], 150° by Sun et al. [124], etc.
- **Organic materials:** Some researchers followed the approach of nature to make superhydrophobic surfaces made from organic materials. One can refer to the works reporting 173° on polyethylene by Lu et al. [125], 162° on polystyrene/dimethylformamide composite by Jiang et al. [126], 150° on polyalkylpyrrole by Yan et al. [127], etc.
- **Inorganic materials:** Some inorganic materials also can lead into superhydrophobic surfaces. Some examples are obtained on ZnO (173°) by Saleema et al [128], (151°) by Yang et al. [129] and on TiO<sub>2</sub> (160°) by Feng et al. [130].

### **Making a rough substrate and modifying it with low surface energy materials**

- **Etching and lithography:** Etching is a straightforward and effective way to make rough surfaces. Different etching methods are tried to make roughness, such as plasma etching [131], laser etching [132] and chemical etching [133]. Lithography



(e.g. photolithography, electron beam lithography, X-ray lithography, soft lithography, nanosphere lithography and so on) is a well-established technique for creating large area periodic micro-/nanopatterns. Some examples of using these methods for a systematic study of superhydrophobicity are as follows: Abdelsalam et al. studied the effect of pore size and shape in controlling wetting of gold and showed that the apparent contact angle was independent of the pore diameter over the range 400-800 nm [134], Martines et al. fabricated ordered arrays of nanopillars by using electron beam lithography and found that a forest of hydrophilic/hydrophobic slender pillars was an very effective water-repellent configuration [135], etc.

- Sol-gel processing: Sol-gel processes can be used to fabricate superhydrophobic surfaces from different materials. For instance, Shirtcliffe et al. [136] prepared porous sol-gel foams from organotriethoxysilanes which exhibited superhydrophobicity at certain temperatures, or Hikita et al. [137] used colloidal silica particles and fluoroalkylsilane and obtained a contact angle of 150°.
- Layer-by-layer (LBL) and colloidal assembly: LBL self-assembly is a rich process to make thin film coatings with molecular level control over film thickness. For recent use of LBL process to make rough surfaces, one can refer to works of Shi et al. [138] on gold aggregates or Zhao et al. [139] on silver films among many others.
- Electrochemical and chemical bath deposition (CBD): Electrochemical deposition is extensively reported to prepare superhydrophobic surfaces. For instance, Zhang et al. [140] fabricated dendritic gold clusters, which was formed by electrochemical

deposition onto indium tin oxide or Shirtcliffe et al. [26] prepared a double-roughened copper surface. As an example of CBD, Hosono et al. [141] used this technique to fabricate a nanopin film of brucite-type cobalt hydroxide.

- Other methods: There are also some other methods for making superhydrophobic surfaces, such as electrospinning [121] and chemical or physical vapour deposition (CVD or PVD) [142].

Several superhydrophobic materials have been produced using a range of chemical and physical methods [143-145]. Some of these coatings show promises of hindering snow accumulation too [146,147]. Figure 2.11 shows two type of the ordered surface morphologies prepared by photolithography method on silicon [95] and polystyrene [148] which are used for superhydrophobicity investigations.

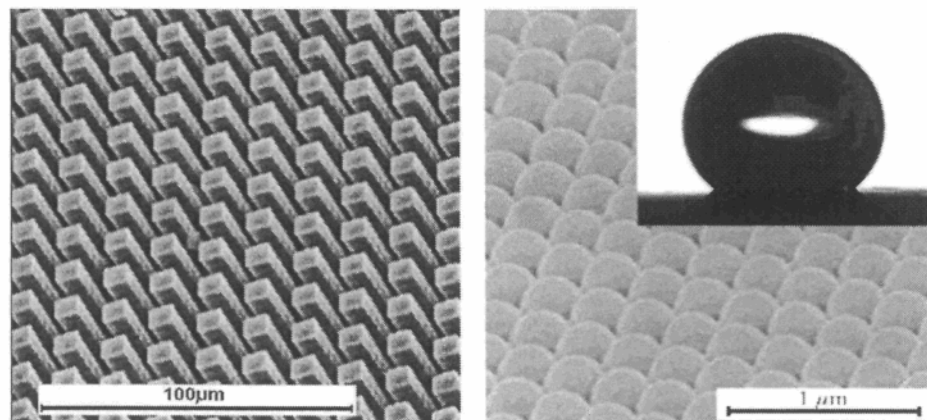
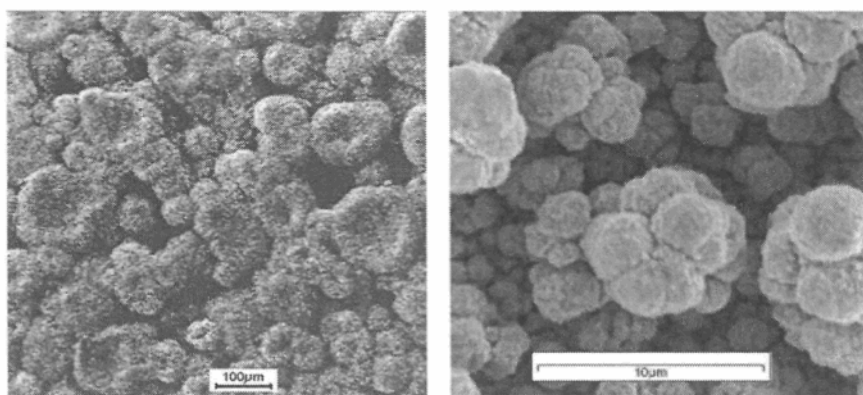


Figure 2.11 : Ordered nanostructures of silicon (left) and polystyrene (right) for superhydrophobicity studies [95,148].

Although the ordered micro/nano structures are extremely valuable to study the details of water droplet behaviour on superhydrophobic surfaces, the regularity of tiny arrangements is not necessary to have high degrees of water repellency; not-ordered rough surfaces can exhibit very similar properties. Figure 2.12 depicts two examples of not-ordered alkylketene dimer [143] and copper [26] superhydrophobic surfaces.



**Figure 2.12 : SEM images of alkylketene dimer (left) and copper (right) surfaces.**

Ideally, a coating layer must be able to: cover the entire surface to give a uniform defect-free layer; bond strongly to the surface; be durable and demonstrate stable performance, and be easy to apply on different substrate shapes, among other criteria. Among the methods mentioned earlier, making the required roughness by spreading the previously prepared nanoparticles is a flexible technique which can be used to make wide range of surfaces in a controlled way. The related aspects of nanoparticles are discussed with more details in the next section.

## ***2.3 Nanoparticles and Their Morphology***

### **2.3.1 Nanoparticles**

Nanomaterials, with at least one of three dimensions in the range of 1 to 1000 nm, have attracted ever-growing interest due to their fascinating properties. Nanoparticles are solid materials with all the dimensions varying in nanometre scale [31,32]. The properties of nanomaterials lie between those of molecules and bulk structures, strongly dependent on the size, shape and structure [149]. In nanometre range, which is typical motion scale of the electron that determines the properties of material, the situation is unique. Nanosize-effects are evident in specific optical, electrical, magnetic and catalytic behaviours quite different from those of the bulk material. In metals, high surface/volume ratio leads to dominant surface effects and nano-particles gain new properties. In noble metals, which have low electrical resistance, the collective oscillations of electrons can be quite strong in the frequency range of ultraviolet and visible light. This appears in special absorption/radiation spectra of noble nanoparticles, for example nanoparticles of gold or silver.

Over the last two decades there have been dramatic advancements in the study of nanomaterials, which have wide applications in electronics [150,151], catalysis [152], biosensors [153], antimicrobial [154], nonlinear optics [155], magnetic storage [156], etc., and many other applications are expected to benefit of nanomaterials in coming years.

### 2.3.2 Preparation of Nanoparticles

The research on the properties of the nanomaterials largely rests on the development of new preparation methods. In general, the various methods of producing nanoparticles can be classified in two broad categories. Figure 2.13 depicts these two categories.

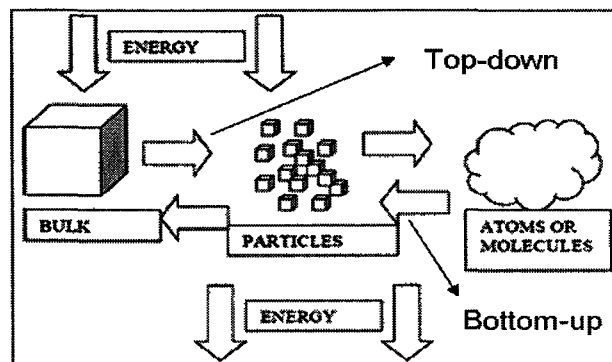


Figure 2.13: Top-down and bottom-up approaches to achieve nanoparticles.

- The “top-down” or “phase-breakdown” procedures are based on breaking down the bulk materials into smaller particles with dimensions in the range of micrometers or nanometres.
- In the “bottom-up” or “phase build-up” approaches, the nanoparticles are synthesized from atoms or molecules as building blocks by chemical reactions [157].

For the case of metals, the phase-breakdown method is based on applying energy to the bulk material in order to separate the pieces of metal, for example by mechanical milling or by fast cooling of molten droplets of metal. These procedures can not provide uniform or monodispersed particles. The focused ion beam (FIB) is another tool which can cut away (mill) pieces with dimensions of microns from a target material and it is possible to operate

directly on the nanoparticles [158]. Milling is achieved by accelerating focused ions, such as gallium ions, to a specific target, which etches off exposed surface of material, ejecting tiny particles. Although this method is very precise, it is expensive and hard to use.

In the bottom-up or “phase build-up” methods, the metallic particles are prepared directly from the metal atoms. This process can be performed either in gas or liquid phase, by controlling the process in liquid medium is easier [157]. The liquid medium synthesis is easier to monitor and control, needs less expensive facilities and materials, and is more appropriate for laboratory scale investigations. Herein, the bottom-up approach is used throughout this text.

Nanomaterials also have different shapes and morphologies. Figure 2.14 depicts some images of silver nanostructures reported in the literature: nanocubes [159], triangular nanoplates, a cross section of nanowires with pentagonal shape and nearly spherical nanoparticles [160].

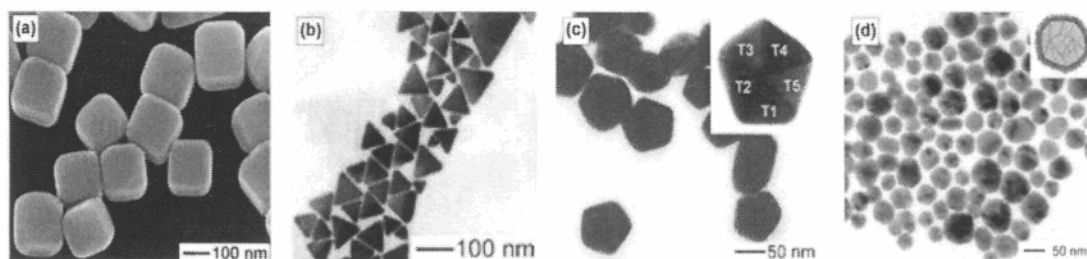


**Figure 2.14: Nanosize silver in different shapes: (a) SEM image of nanocubes, TEM image of triangular nanoplates (b), pentagonal cross section of nanowires (c) and nearly spherical nanoparticles.**

The size, shape and structure of nanomaterials are dependent to great extent on the selected preparation method and its parameters such as reagent concentrations, temperature, time, etc. Figure 2.15 shows the drastic change in the morphology by doubling the concentration of one of the reagent in the reaction [161].

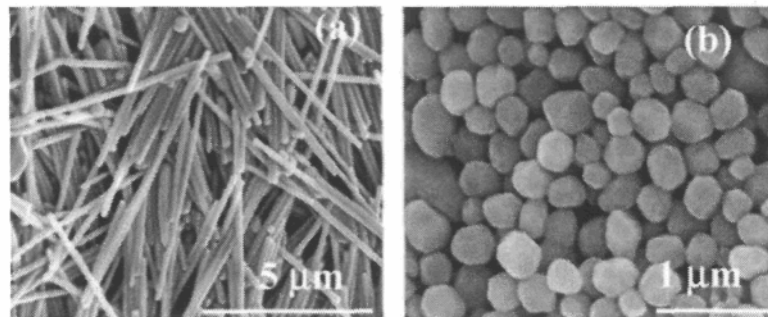


Figure 2.15 : SEM images of silver nanorods (a) and nanoparticles (b) [161]

### 2.3.2 Nanoparticle-based Coatings

As described previously, some degree of surface roughness is needed to achieve superhydrophobicity. It is common to use the nanoparticles not only in colloidal solutions but also in solid phase. Spreading the nanoparticles onto a solid surface can provide new surface morphologies with nanosize roughness. Different approaches have been reported to bring and bind the nanoparticles onto the surfaces to make them rough. For instance, silica particles have been coated on latex by sol-gel processing [162] or on glass by dip-coating [163]. Another example is  $\text{TiO}_2$  nanoparticles by spray coating on cement [164] or glass [165]. There are very few articles about this application of metallic nanoparticles, such as [166,167], but apparently there is rarely any report of making the metallic nanoparticles and

bringing them onto the surface toward achieving superhydrophobicity. Figure 2.16 shows the rough surfaces with high degree of superhydrophobicity prepared by silica [162] and titanium dioxide [164] nanoparticles. This is the intended approach in this research.

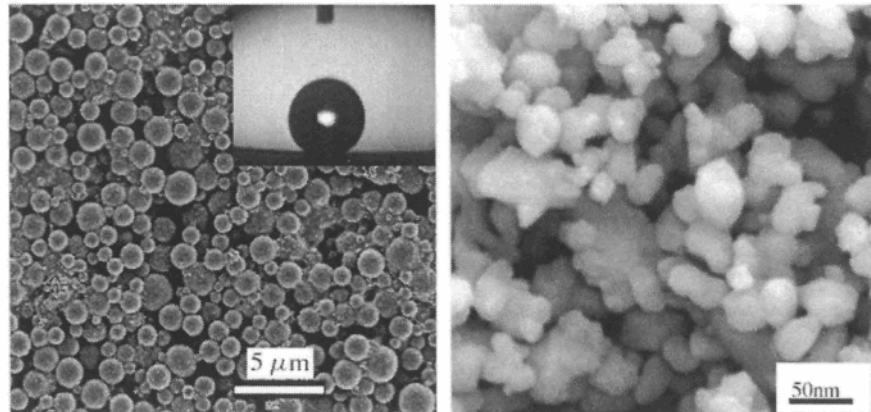


Figure 2.16 : The surface morphology after coating with silica particles (left) or  $\text{TiO}_2$  (right) to achieve superhydrophobic surfaces.